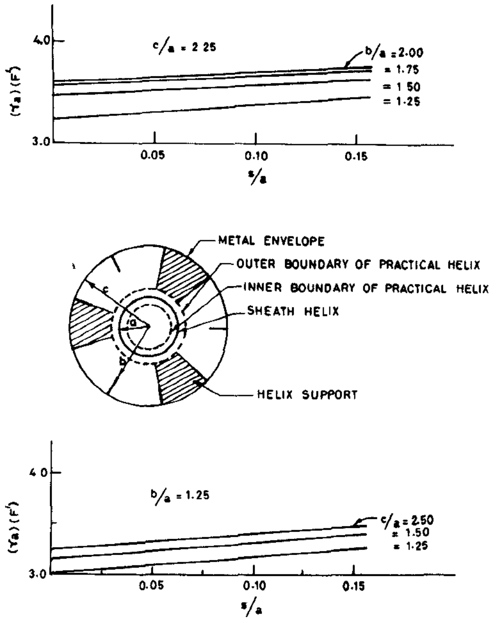

Fig. 1. $(\gamma a)(F')$, a quantity proportional to gain, as a function of the dimensions of the vane-loaded helical structure.

by $\alpha_L \mu_0$ and $\mu_C \epsilon_0$, respectively, in the expression for the impedance parameter F of an identical helix in free space [2]. This would lead to

$$F' = F(\alpha_L/\alpha_C)^{1/6}. \tag{1}$$

The interaction impedance, which is related to the impedance parameter [2], then may be expressed as

$$K' = K(\alpha_L/\alpha_C)^{1/2} \tag{2}$$

where K' represents the interaction impedance of the vane-loaded helix and K represents the corresponding quantity for an identical helix in free space. K may be suitably expressed using the dispersion relation as [2]

$$K = \frac{1}{2}\left[\frac{I_1(\gamma a)K_1(\gamma a)}{I_0(\gamma a)K_0(\gamma a)}\right]^{1/2} F^3 \cot\psi \tag{3}$$

where a is the mean helix radius, ψ is the helix pitch angle, I_n and K_n $(n = 0,1)$ are the modified Bessel functions of the first and the second kinds, respectively, and γ is the radial propagation constant of the structure.

III. Result and Discussion

The various structure dimensions shown in Fig. 1 and Table I are the mean helix radius a, being equal to the sheath helix radius, the radial coordinate of the tips of the vanes b, the radius of the metal envelope c, and the seperation s between the sheath helix and the dielectric supports, being equal to the helix-wire radius.

In Table I, the typical optimized vane-loaded $(b \neq c)$ and vaneless $(b = c)$ structures are compared with respect to the characteristic impedance $Z(= (L/C)^{1/2})$ [1] and the interaction impedance K. It is found (Table I) that the optimized vane-loaded structure is superior to the optimized vaneless structure with respect to having a higher value of the interaction impedance and, hence, the gain and efficiency of the device [2]. Table I also gives the characteristic impedances of these structures and the

TABLE I
The Characteristic and Interaction Impedances of the Optimized Vane-Loaded Structure Compared With Those of the Optimized Vaneless Structure

	$\gamma a = 1.6$; $\cot\psi = 8$		
	Optimised vane-loaded structure:c/a=2.50, s=0;(b/a)opt=1.70	Optimised vaneless structure:b=c,s=0; (c/a)opt=1.25	Helix-in-free-space
$Z_{(Ohm)}$	105.6	62.4	140.6
$K_{(Ohm)}$	53.6	30.9	53.2

corresponding results for an identical helix in free space for the sake of comparison. In Fig. 1, $(\gamma a)(F')$, a quantity proportional to the gain of the device, is plotted against the various structural dimensions, showing qualitatively how the gain of the device would increase with s, b, and c.

References

[1] B. N. Basu, B. B. Pal, V. N. Singh, and N. C. Vaidya, "Optimum design of a potentially dispersion free helical slow-wave circuit of a broad-band TWT," *IEEE Trans. Microwave Theory Tech.*, vol. MTT-32, pp. 461–463, Apr. 1984.
[2] J. R. Pierce, *Travelling-Wave Tubes.* New York. Van Nostrand, 1950, appendix II, pp. 229–232.
[3] S. N. Joshi and B. N. Basu, "Equivalent circuit analysis of a practical slow-wave structure for TWT's," *J. Electron. Telcomm. Eng.*, vol. 25, pp. 423–425, Oct. 1979.

Conversion Losses in GaAs Schottky-Barrier Diodes

OLDWIG VON ROOS and KE-LI WANG

Abstract —**The conversion losses of a Schottky-barrier diode have been calculated for a set of realistic diode parameters. It is found that previous work overestimated the substrate losses by 30 percent. It is also shown that a lightly doped epitaxial layer will decrease the barrier capacitance and with properly designed thickness will avoid any resistance losses due to this layer. Parasitic losses can thus be reduced substantially.**

I. Introduction

The model of a Schottky-barrier diode we contemplate in the present work consists of a cylindrical contact of radius a on a thin cylindrical wafer of n-type semiconductor material possessing a radius $b \gg a$. The semiconductor wafer in turn consists of a layer of undoped or at least lightly doped GaAs epitaxially grown on a heavily doped n-type GaAs substrate several mils thick. Under high-frequency operation, the equivalent circuit of the structure just described consists of a spreading impedance Z_s in series with a combination of the barrier resistance R_b and the barrier capacitance C in parallel [1]. The current–voltage characteristic for a small ac signal may then be represented by

$$I = \frac{1 + i\omega C R_b}{R_b + Z_s + i\omega C R_b Z_s} V. \tag{1}$$

Manuscript received April 8, 1985; revised July 8, 1985. This work was supported in part by JPL Director's Discretionary Fund.
The authors are with the Jet Propulsion Laboratory, California Institute of Technology, 4800 Oak Grove Dr., Pasadena, CA 91109.
IEEE Log Number 8405821.

It can be shown [1] that the parasitic loss of the device, defined as the ratio of the total power absorbed to the power available to the barrier resistance alone, is given by[1]

$$L = 1 + R_s/R_b + \omega^2 C^2 R_s R_b \tag{2}$$

where R_s signifies the real part of Z_s, the spreading impedance. It is the aim of the designer to keep L as small as possible, which can obviously be achieved by minimizing R_s and C. In the following, we shall give a re-evaluation of the spreading resistance based on the theory given by Dickens [2], taking due account of the influence of the scattering frequency and displacement currents on the conductivity [3]. An account of the barrier capacitance provided by a GaAs epitaxial layer will also be given.

II. The Spreading Resistance R_s

According to the theory developed by Dickens [2], the impedance of current flowing through a small circular disk into a substrate consisting of a homogeneously doped semiconductor is given by [2, eq. (62)]

$$Z_s = \frac{i\omega\mu_0}{2\pi\gamma}\int_0^{\xi_1}\xi d\xi(\xi^2+1)^{-1}\left(1+\frac{e^{-a\gamma\xi}}{\sin(a\gamma)\xi}\right) \tag{3}$$

where $\xi_1 = b/a \gg 1$ is the ratio of the outer radius of the substrate to the radius of the disk, which in our case constitutes the Schottky contact, ω is the angular frequency, μ_0 the permeability of free space, and γ, the propagation constant, is given by

$$\gamma = (i\omega\mu_0)^{1/2}(\sigma + i\omega\epsilon\epsilon_0)^{1/2}. \tag{4}$$

In (4), ϵ signifies the relative dielectric constant, ϵ_0 the permittivity of free space, and the conductivity σ is given by [3]

$$\sigma \frac{\sigma_0}{1+i\omega\tau} \tag{5}$$

where τ is the average time between collisions of the majority carriers [4]. The connection between σ_0 and τ is given by the mobility μ via

$$\sigma_0 = q\mu N \qquad \mu = \frac{q\tau}{m^*} \tag{6}$$

where N is the carrier density, m^* the effective mass, and q the elementary charge. The model underlying (5) and (6) is a rather simple one but sufficiently accurate for our purposes.

If we assume for a moment that the absolute value of $a\gamma$ is very small, then (3) shows that

$$Z_s \to \frac{i\omega\mu_0}{2\pi\gamma}\ln(b/a) + \frac{i\omega\mu_0}{2\pi a\gamma^2}\tan^{-1}(b/a) \tag{7}$$

in this case. The first term on the RHS of (7) is attributed to the skin effect and the second term to the spreading resistance. It can be easily shown that (7) is identical with the corresponding expressions given in [3] and [5]. But the quantity $a\gamma$ is for many realistic cases far from small, and replacing the exponential in the integrand of (3) by unity constitutes a serious mistake. With the definition

$$a\gamma = z = z_1 + iz_2 \tag{8}$$

the integral (3) becomes

$$Z_s = \frac{i\omega\mu_0 a}{2\pi}\left\{\frac{\ln(b/a)}{z} + \frac{f(z)}{z\sin z}\right\} \tag{9}$$

[1]There are other losses (for instance, losses associated with impedance mismatch at the RF and IF ports) if the device is used as mixer. We do not contemplate these additional losses here.

with

$$f(z) = ci(z)\sin(z) - si(z)\cos(z) \tag{10}$$

where[2]

$$ci(z) = C + \ln z + \int_0^z \frac{\cos t - 1}{t}dt \tag{11a}$$

is the integral cosine and

$$si(z) = -\frac{\pi}{2} + \int_0^z \frac{\sin t}{t}dt \tag{11b}$$

the integral sine.

Because of the assumption $b/a \gg 1$, we have extended the integration over the exponential part of the integral (3) to infinity without loss of accuracy. We recuperate (7) from (9) for small absolute z since $\lim f(z) = \pi/2$ and $\tan^{-1}(b/a) = \pi/2$ for large b/a. It is of interest to evaluate Z_s in the low- and high-frequency limit. In the low-frequency limit $\omega \to 0$, we have from (4) and (8)

$$z = (1+i)a(\omega\mu_0\sigma_0/2)^{1/2} \tag{12}$$

so that $z_1 = z_2 \ll 1$. Equation (9) reveals then that for $\omega \to 0$

$$Z_s = \frac{1+i}{4\pi}\left(\frac{2\mu_0\omega}{\sigma_0}\right)^{1/2}\ln(b/a) + \frac{1}{4a\sigma_0} \tag{13}$$

identical with the classical result [2]. In the high-frequency limit $\omega \to \infty$, we have from (4) and (5) that

$$z = i\omega\sqrt{\epsilon}\,a/c = iz_2. \tag{14}$$

But for large absolute z ($\arg z < \pi$), we also have for $f(z)$ [6, eq. (10)] $f(z) = z^{-1}$ and therefore ($\epsilon = 1$ in this case)

$$Z_s = \frac{\mu_0 c}{2\pi}\ln(b/a) + \frac{\mu_0 c^2}{\pi\omega a}e^{-\omega a/c} \approx \frac{\mu_0 c}{2\pi}\ln(b/a) \tag{15}$$

independent of frequency.

For most semiconductor material of interest in this context and for frequencies ν above 100 GHz but below 30 THz, it turns out that the absolute value of z is less than 2. We assume throughout a value of the order of 1 μm for the radius of the contact disk. In this case, $f(z)$, as well as the trigonometric functions occurring in the expression for Z_s, (9), can be expanded in powers of z and it is sufficient to go to order $0(z^5)$. Since we are interested only in the real part of Z_s according to (2), we will give the result of the expansion of (9) only for the real part of Z_s, or the spreading resistance R_s. With the definition

$$r = (z_1^2 + z_2^2)^{1/2} \tag{16}$$

we have

$$\begin{aligned} R_s = \frac{\omega\mu_0 a}{2\pi}\Bigg\{ & \frac{z^2}{r_2}\ln(b/a) + \pi\frac{z_1 z_2}{r^4} - (1-C)\frac{z_2}{r^2} \\ & + \frac{z_2}{r^2}\ln r - \frac{z_1}{r^2}\sin^{-1}(z_2/r) \\ & - \frac{5}{36}z_2 + \frac{\pi}{45}z_1 z_2 - \frac{269}{7200}z_1^2 z_2 \\ & + \frac{269}{21600}z_2^3 + \frac{4\pi}{945}z_1 z_2(z_1^2 - z_2^2)\Bigg\} \end{aligned} \tag{17}$$

valid for $r < 2$. From the defining equations for z, (8) and (4), we

[2]$C = 0.577216$ is Euler's constant.

obtain

$$z_1 = \frac{a}{2}\sqrt{\omega\mu_0}(\alpha - \beta) \tag{18a}$$

$$z_2 = \frac{a}{2}\sqrt{\omega\mu_0}(\alpha + \beta) \tag{18b}$$

where

$$\alpha = \left(A + \sqrt{A^2 + B^2}\right)^{1/2} \quad \beta = B/\left(A + \sqrt{A^2 + B^2}\right)^{1/2} \tag{19}$$

and A and B are in turn given by

$$A = \frac{\sigma_0}{1 + \omega^2\tau^2} \quad B = \omega\left(\epsilon\epsilon_0 - \frac{\sigma_0\tau}{1 + \omega^2\tau^2}\right). \tag{20}$$

Equation (17) represents the spreading resistance of the substrate within the limits indicated ($r < 2$). This is to be compared with the usual expression given by previous authors [3], [5] who retain only the first two terms in the braces of (17). As an example of the error introduced in this way, let us compute R_s with the following values of the parameters which determine z_1 and z_2. $\sigma_0 = 10^5$ mho m^{-1}, $\epsilon = 10.8$, $\tau = 10^{-13}$ s, $a = 1$ μm, $b = 50$ μm, and $\nu = 12\,000$ GHz. In this typical case, the absolute value of z turns out to be $r = 0.759$, well within the range of the validity of (17) but certainly not small compared to unity. We obtain $R_s = 17.4$ Ω. However, the value for R_s obtained from the incorrect (7) is $R_s = 23$ Ω, an overestimate by 30 percent.

An undepleted epitaxial layer will also contribute to the spreading resistance [5]. But if the epilayer is judiciously grown and doped, the depletion layer underneath the Schottky barrier can be extended to the substrate and the epilayer resistance avoided (Mott barrier). This idea leads directly to a consideration of the barrier capacitance.

III. The Barrier Capacitance

The width of the depletion layer within an epitaxial layer of thickness t just underneath a Schottky-barrier contact is given by

$$W = \sqrt{\frac{2\epsilon\epsilon_0}{qN_D}(V_b - V)} \tag{21}$$

if $W \leqslant t$. Here N_D signifies the number density of donors, V_b the barrier height as seen from the semiconductor, and V is the applied (forward) voltage. The barrier capacitance C follows from (21) in a well-known manner [3], [7] and is in turn given by

$$C = \frac{\epsilon\epsilon_0}{W}\pi a^2. \tag{22}$$

V_b is connected to the barrier height proper ϕ_b, the discontinuity at the metal–semiconductor interface, via

$$V_b = \phi_b + kT\ln(N_D/N_c) \tag{23}$$

where N_c is the density of states of the conduction band. A heuristic connection between ϕ_b and the band-gap energy E_G is given by the "two-thirds rule," i.e. [8],

$$\phi_b = \frac{2}{3}E_G. \tag{24}$$

To minimize losses, C must be made small according to (2). This means that for a given contact radius a, the depletion layer width W must be made large. This can obviously be achieved by decreasing the dopant concentration N_D according to (21). If the thickness of the epitaxial layer t is larger than the space-charge layer width W, a contribution to the spreading resistance due to the undepleted epilayer between the space-charge layer and the heavily doped substrate will arise. But this contribution to R_s will be large because of the low conductivity of the lightly doped material. If, however, the space-charge layer can be extended into the substrate, no such resistance contribution arises as far as the ac current is concerned, since it is supported entirely by displacement currents in the space-charge region.

TABLE I
List of Parameter Values for the Determination of the Barrier Capacitance

$N_1 = 1 \times 10^{14}$ cm^{-3}
$N_c = 4.7 \times 10^{17}$ cm^{-3}
$N_2 = 2 \times 10^{18}$ cm^{-3}
$\epsilon = 10.8$
$t_1 = 1$ µm
$E_G = 1.43$ eV
$\Delta_1 = 0.074$ eV

Suppose, we have a layer of semiconductor 1 possessing a uniform doping concentration N_1, a dielectric constant ϵ_1, and thickness t_1 grown on a layer of semiconductor 2 possessing a doping concentration N_2, a dielectric constant ϵ_2, and thickness t_2. It can then be shown by solving Poisson's equation that the depletion-layer thickness becomes

$$W_{\text{eff}} = \left(1 - \frac{\epsilon_2}{\epsilon_1}\right)t_1 + \left\{\frac{2\epsilon_2\epsilon_0}{qN_2}(V_{b1} - V) + \frac{\epsilon_2}{\epsilon_1}\left(\frac{\epsilon_2}{\epsilon_1} - \frac{N_1}{N_2}\right)t_1^2\right\}^{1/2}. \tag{25}$$

Here, V_{b1} is given by the equation

$$qV_{b1} = q\phi_b + \Delta_1 \tag{26}$$

where Δ_1 is the energy difference between the quasi-Fermi level and the conduction band edge of the substrate, a positive quantity for heavily doped degenerate material. Equation (25) is of course valid only if $t_1 < W_{\text{eff}}$, otherwise the space-charge layer would not penetrate the substrate. Since $\epsilon_1 = \epsilon_2 = \epsilon$ in our case, we obtain from (25)

$$W_{\text{eff}} = \left(\frac{2\epsilon\epsilon_0}{qN_2}(V_b - V) + \left(1 - \frac{N_1}{N_2}\right)t_1^2\right)^{1/2}. \tag{27}$$

In order that $t_1 < W_{\text{eff}}$, the inequality

$$\frac{2\epsilon\epsilon_0}{q}(V_b - V) > N_1 t_1^2 \tag{28}$$

must be satisfied. Using the parameter values of Table I, we find that the voltage across the barrier must be larger than 0.084 V in order for the unequality (28) to hold. In this case, (27) reveals that $W_{\text{eff}} \not\equiv t_1$ and the barrier capacitance now becomes

$$C = \frac{\epsilon\epsilon_0}{t_1}\pi a^2 = 9.56 \times 10^{-5}\pi a^2 [F]. \tag{29}$$

Usually, the epilayer is doped more heavily than indicated in Table I of our example. For $N_1 = 2 \times 10^{17}$ cm^{-3} as reported in the literature [5], the barrier capacitance becomes an order of magnitude larger than the value quoted in (29) with a concomitant

TABLE II
LIST OF PARAMETER VALUES FOR THE DETERMINATION OF THE SPREADING RESISTANCE AND PARASITIC LOSSES OF THE SUBSTRATE

$\sigma_0 = 10^5$ A/Vm
$\tau = 10^{-13}$ s
$\varepsilon = 10.8$
$R_b = 200\ \Omega^{*)}$
$C = 3 \times 10^{-16}$ F
$a = 1\ \mu$m
$b = 50\ \mu$m

*This value was determined from the thermionic theory [7] using a forward bias of $V = 0.893$ V. At this bias, the inequality (28) is still valid. $T = 300$ K.

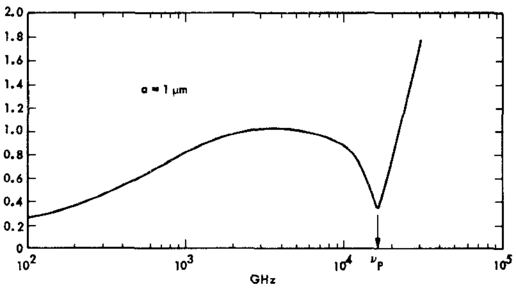

Fig. 1 The absolute magnitude r of the propagation constant $a\gamma$, (4), as a function of frequency. Parameter values used for the computation are given in Table II. ν_P is the plasma frequency

larger loss according to (2) at higher frequencies. It is therefore advantageous to use a less heavily doped epilayer, provided that the space-charge layer extends into the substrate as discussed above.

IV. RESULTS

We have calculated the spreading resistance R_s as a function of frequency using either the correct equation (17) or the real part of (7). The latter expression has been used previously for the determination of R_s [3], [5]. But we have shown that this is only permissible if the quantity z, (8), is small compared to one. Typical values for the conductivity and collision frequency of heavily doped n-type GaAs are $\sigma_0 = 10^5$ mho m^{-1} and $\tau = 10^{-13}$ s, respectively. These values lead to an electron mobility of $\mu = 0.26$ m^2/Vs according to (6), assuming an effective mass of 0.067 electron masses. Using the values quoted here and also listed in Table II, we have calculated the absolute value r of the propagation constant z, (12), as a function of frequency above 100 GHz. The results are shown in Fig. 1 for a contact radius of $a = 1$ μm. As can be seen, the magnitude of r is certainly far from being small compared to one. We also notice a sharp dip of the magnitude of r at a frequency of 16 THz. This resonance frequency corresponds to the classical plasma frequency and the minimum of r at that frequency translates into a maximum for R_s at the same frequency. The plasma frequency ν_P is well

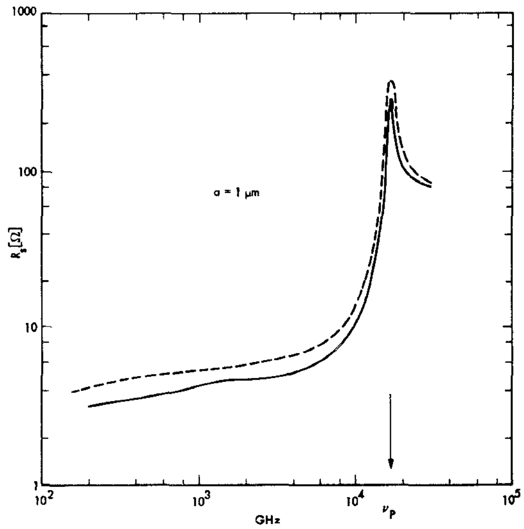

Fig. 2. The spreading resistance as a function of frequency. Both curves are computed using the parameter values listed in Table II The solid curve is based on (17) and the dashed curve represents R_s obtained from the real part of (7).

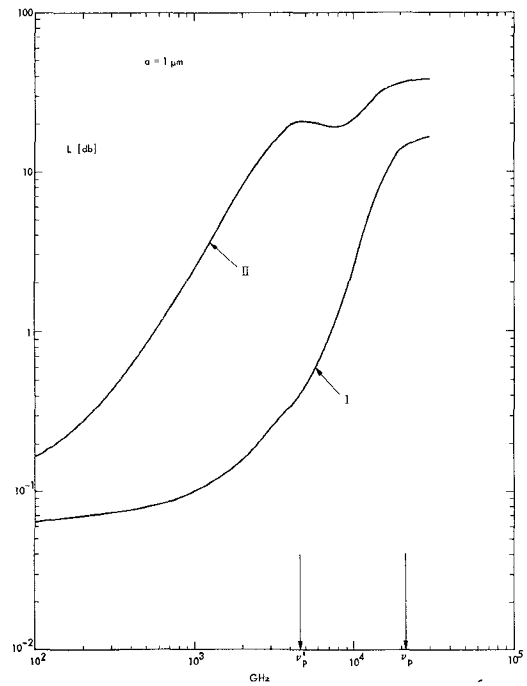

Fig. 3. The parasitic loss L, (2), as a function of frequency. Curve I represents the loss computed for the model proposed in this work Curve II represents the loss computed for a conventional model. ν_P' signifies the plasma frequency of the epilayer, and ν_P the plasma frequency of the substrate. See text for details.

known to be

$$\nu_P = (2\pi)^{-1}\left(q^2 N_D/\epsilon\epsilon_0 m^*\right)^{1/2} = (2\pi)^{-1}\left(\sigma_0/\epsilon\epsilon_0\tau\right)^{1/2} \quad (30)$$

an expression which yields indeed 16 THz when using the values for the parameters entering (30) listed in Table II. Fig. 2 shows the spreading resistance R_s as a function of frequency. The solid curve represents R_s as computed with the help of (17) and the dashed curve represents the real part of (7), i.e., the expression for R_s used by previous authors [3], [5]. Almost throughout the range of frequencies contemplated, the incorrect spreading resistance, the dashed curve of Fig. 2, is 29 percent larger than the

TABLE III
LIST OF PARAMETER VALUES FOR THE DETERMINATION OF THE RESISTANCE OF THE UNDEPLETED EPILAYER

σ_0 = 12800 A/Vm
$\tau = 1.55 \times 10^{-13}$ s
$N_1 = 2 \times 10^{17}$ cm^{-3}
$C = 4 \times 10^{-15}$ F

correct one, the solid curve of Fig. 2. It is of course true that for low frequencies ($\nu < 100$ GHz), as well as for very high frequencies ($\nu > 30$ THz), the "wrong" expression for R_s, (7), merge with the correct expression (3) as discussed in Section II. However, it is remarkable that the two expressions, either the real part of (7), or (17) (valid for $r < 2$), give the same trend as a function of frequency, one merely being shifted by an almost constant amount of some 30 percent upward from the other within the frequency range of interest (100 GHz $< \nu <$ 30 THz).

With the values as given in Table I, we have also calculated the loss L, (2), as a function of frequency using the values of R_s from Fig. 2. These are shown in Fig. 3 as curve I. It can be seen that the resonance at the plasma frequency ν_P has disappeared in favor of an abrupt change in slope due to the frequency-dependent term of (2). As the frequency increases above ν_P, the resistance R_s decreases but not as fast as the square of the frequency increases. We also see that below 2000 GHz = 2 THz, the parasitic losses are fairly small for our model.

We now discuss curve II of Fig. 3. Here, we have plotted the loss L, (2), using a model found in the literature [5]. The epilayer consists of GaAs doped to $N_1 = 2 \times 10^{17}$ cm^{-3}. Table III lists the corresponding values for the dc conductivity and collision time found from (6) and the capacitance of the epilayer as given by (21) and (22). The undepleted epilayer thickness t was assumed to be $t = 0.125$ μm [5]. The epilayer reisistivity becomes

$$R_{\text{epi}} = \frac{2}{\pi} t \omega \mu_0 \frac{z_1 z_2}{\left(z_1^2 + z_2^2\right)^2} \tag{31}$$

where z_1 and z_2 are defined by (8) and (18)–(20). The values of σ_0 and τ to be used are those of Table III. In order to determine the loss, (2), R_{epi} of (30) must be added to the substrate resistance of Fig. 2, and finally the capacitance to be used must be computed from (21) and (22) with $N_D = N_1 = 2 \times 10^{17}$ cm^{-3}, the dopant concentration of this model [5]. The result is shown by curve II of Fig. 3. As can be seen, the parasitic losses are larger for this model than they are for the case of the lightly doped epilayer with "punch through" of the space-charge layer as discussed above. The reason is twofold. At low frequencies (below 2 THz), R_{epi} is about as large as R_s, given the parameter values of Tables II and III. At high frequencies where R_{epi} becomes negligibly small,[3] the frequency-dependent term of (2) dominates and the loss L becomes proportional to C^2. Since the ratio of the capacitances underlying the model of curve II (Fig. 3) and that of curve I (Fig. 3) is about 13, simply because of the difference in doping level $N_1 = 2 \times 10^{17}$ cm^{-3} for the model culled from the literature [5] and $N_1 = 5 \times 10^{14}$ cm^{-3} for our

[3]It can easily be shown from (4), (5), and (8) that $z_1 \sim \omega^{-2}$ for high frequencies and thus R_{epi} goes to zero in this limit according to (30).

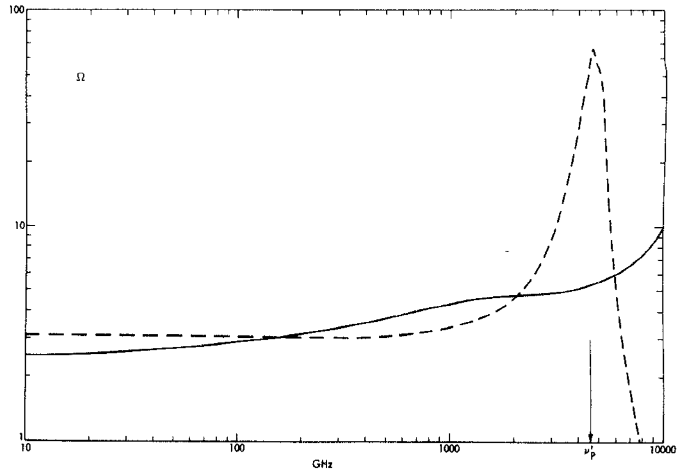

Fig. 4. A comparison of the spreading resistance R_s of the substrate (solid curve) with the resistance of the undepleted epilayer R_{epi} (dashed curve) for the conventional model adopted in the text.

"punch through" configuration as amply explained in Section III, we see that at high frequencies (above 10 THz) the difference between curve II and curve I of Fig. 3 is approximately a constant 22 dB. The point of inflection at 4600 GHz of curve II is easily explained when looking at Fig. 4. To clarify, we plotted both the spreading resistance of the substrate form Fig. 2 on Fig. 4 (solid curve) together with the resistance of the undepleted epilayer of the conventional model (dashed curve). We see, that the resistance of the epilayer and that of the substrate are more or less equal below 2 THz, but the resistance of the epilayer shows a sharp maximum at $\nu = \nu_P' = 4.7$ THz. This resonance is analogous to the resonance shown in Fig. 2 for the substrate's resistance and occurs again at the plasma frequency given by (30) but now using the parameter values of Table III for its computation. Beyond the peak, R_{epi} drops quickly to very small values as the frequency is increased, and this is the origin of the point of inflection of curve II of Fig. 3 in the neighborhood of ν_P'.

V. CONCLUSION

We have shown, that the spreading resistance of the substrate of a Schottky-barrier diode is reduced by some 30 percent from values quoted in the literature [3], [5] when calculated correctly. A contribution toward the resistance due to an undepleted epitaxial layer can be avoided by carefully tailoring the space-charge layer and at the same time the barrier capacitance can be reduced appreciably.

Thus, parasitic losses can be reduced by between 1 to 25 dB from conventional diode structures depending on the frequency.

REFERENCES

[1] G. C. Messenger and C. T. McCoy, "Theory and operation of crystal diodes as mixers," *Proc IRE*, vol. 45, pp. 1269–1283, Dec. 1957.
[2] L. E. Dickens, "Spreading resistance as a function of frequency," *IEEE Trans. Microwave Theory Tech.*, vol. MTT-26, pp. 101–109, Feb. 1967.
[3] K. S. Champlin and G. Eisenstein, "Cutoff frequency of submillimeter Schottky-barrier diodes," *IEEE Trans. Microwave Theory Tech.*, vol. MTT-26, pp. 31–34, Jan. 1978.
[4] K. S. Champlin, D. B. Armstrong, and P. D Gunderson, "Charge carrier inertia in semiconductors," *Proc. IRE*, vol. 52, pp. 677–685, June 1964.
[5] W. M. Kelly and G. T. Wrixon, "Conversion losses in Schottky-barrier diode mixers in the submillimeter region," *IEEE Trans. Microwave Theory Tech.*, vol. MTT-27, pp. 665–672, July 1979.
[6] M. Abramowitz and I. E Stegun, *Handbook of Mathematical Functions*. New York: Dover Publications, 1965, p. 233.
[7] S. M. Sze, *Physics of Semiconductor Devices*. New York: Wiley-Interscience, 1969, pp. 371, 378–381.
[8] R. Stirn, "Dependence of barrier height on energy gap in Au n-type $GaAs_{1-x}P_x$ Schottky diodes," *Appl. Phys. Commun.*, vol. 1, pp. 43–53, Apr. 1981.